Aluminum Nanoparticle Modeling in Sentaurus Device

Abstract

In understanding the physics properties of nano-structure provided by Doctor Dirk Weiss in Washington Technology Center (WTO), I designed a Sentaurus program, which uses TCAD Sentaurus mobility degradation models for the simulation of devices containing high-k dielectric materials like Aluminum nanoparticles. The model parameters are calibrated to fit experimental data in the first part of the project. In the second part, a variation of the characteristics of the 45-nm CMOS technology node due to the use of high-k mobility degradation is considered.

I. Introduction

High-k insulators such as AlPO are to be utilized as gate dielectric films for advanced CMOS devices. One of main problems of the high-k MISFETs is reduced carrier mobility compared with that of thermally grown pure SiO_2 MOSFETs, since lower carrier mobility degrades the device performance. There are two sources of the mobility degradation; one is Coulomb scattering caused by fixed charges in AlPO films and the other is phonon scattering by interfacial thin Si-AlPO layer; and AlPO-related remote phonon scattering is not dominant. The mobility degradation caused by the Coulomb scattering and AlPO phonon scattering is separated into two components and we develop an empirical mobility model for AlPO devices that enables accurate simulation of electrical characteristics of the AlPO devices.

II. Mobility Reduction

1. Matthiessen's rule:

$$\frac{1}{\mu_{AlPO}} = \frac{1}{\mu_{Si_3N_4}} + \frac{1}{\Delta\mu} \tag{1.1}$$

where μ_{AlPO} is the effective mobility for AlPO devices, $\mu_{Si_3N_4}$ is the effective mobility for Si_3N_4 devices and $\Delta\mu$ is the mobility reduction caused by the AlPO gate insulators compared with the Si_3N_4 films. The mobility degradation $\Delta\mu$ is proportional to the power of N; $\Delta\mu \propto N^{\alpha}$ with N being the inversion electron density; and the slope a strongly depends on the temperature and the substrate acceptor concentration.

2. Dependence of the mobility degradation $\Delta\mu$ on electron sheet density N and temperature T:

(1). Remote Coulomb scattering (RCS):

$$\mu_c \propto N^{\alpha_C} \tag{1.2}$$

(2). Remote phonon scattering (RPS):

$$\mu_P \propto N^{\alpha_P} \tag{1.3}$$

Where α_C and α_P weakly depend on T.

(3). Difference between α_C and α_P:

The RCS-limited mobility becomes higher at strong inversion condition and at higher temperature, since screening effect becomes larger at higher carrier density and at higher temperature. In contrast, the RPS-limited mobility becomes lower at strong inversion condition and higher temperature, since phonon-electron interaction becomes stronger under higher electric field and at higher temperature.

III Effective mobility of a AlPO gated nMOSFET.

At low fields, the effective mobility of the AlPO sample is significantly lower than that of the SiO2 sample, which may be attributed to the much stronger Coulomb scattering for the former due to its much higher trapped charge density (include interface traps, border traps and bulk traps), as well as fixed oxide charge density. Here the Coulomb scattering includes possible remote coulomb scattering RCS due to charges at some distances away from the dielectric/substrate interface. It's because in the low-field regime, the effective mobility is approximately linearly proportional to the inversion charge density, which is consistent with the carrier screening effect.

In addition to Coulomb scattering caused by high densities of charges, the scattering caused by high densities of charges, the scattering due to soft optical phonons in high-k dielectrics is an intriguing possibility that cannot be overlooked. To analyze the possible phonon scattering effect, we can modify Matthiessen's rule:

$$\frac{1}{\mu_{ph}} = \frac{1}{\mu_{eff}} - \frac{1}{\mu_{coul}} - \frac{1}{\mu_{sr}} \tag{1.4}$$

Where μ_{eff} is the total effective mobility, μ_{coul} is the mobility limited by Coulomb scattering, and μ_{sr} is the mobility limited by surface roughness.

IV Soft optical phonon scattering

The scattering rate by the soft optical phonons in AlPO is a relatively weak function of temperature. The weak temperature dependence of the scattering rate for soft optical phonon can be qualitatively explained by he following derivation. In the two dimensional deformation potential theory of surface phonon scattering, the scattering rate due to optical phonon may be expressed as:

$$\frac{1}{\tau_{op}} \propto [N_R + (N_R + 1)u(E - \hbar\omega)] \tag{1.5}$$

Where $N_R = 1/(e^{\frac{\hbar\omega}{kT}} - 1)$ is the phonon occupation number, E is the carrier energy, ω is the phonon frequency, and u (x) is the unit step function, u (x<0) = 0 and u (x>0) = 1. Assume that the phonon energy is smaller than the thermal carrier energy, i.e., $\hbar\omega < E$, then:

$$\frac{1}{\tau_{op}} \propto (2N_R + 1) = \frac{e^{\frac{\hbar\omega}{kT}} + 1}{e^{\frac{\hbar\omega}{kT}} - 1} \tag{1.6}$$

This question indicates that when $\hbar\omega << kT, \frac{1}{\tau_{op}} \propto T$, and when $\hbar\omega > kT, \frac{1}{\tau_{op}}$ approaches a constant, i.e. independent of temperature.

V Sentaurus Workbench structure

The Sentaurus Workbench project is split into two parts. In the first part of the setup, the model parameters are calibrated and the results of the experimental findings of are reproduced. The second part of the project repeats the setup used in the technology template. It uses the model parameters obtained in the first part. The device characteristics with and without the use of the high-k models are obtained and compared.

1. Part I: High-k model parameter calibration.

In this part of the project, the high-k model parameters are calibrated in such a way that the electron mobility as a function of the electrical field matches the experimental results given by Doctor Dirk Weiss. The simulation is organized as a Sentaurus Workbench project. The tool flow of the project is like:
Sentaurus Structure Editor -> Sentaurus Device -> Inspect

(1). Sentaurus Structure Editor:

A simple two-dimensional (2D) flat structure consisting of a Si_3N_4 top layer, a silicon substrate, a following Si_3N_4 interface layer, and an AlPO grid layer between electrical contacts is created using the standard commands of Sentaurus Structure Editor. The acceptor concentration in the silicon is

set to $10^{16} cm^{-3}$.

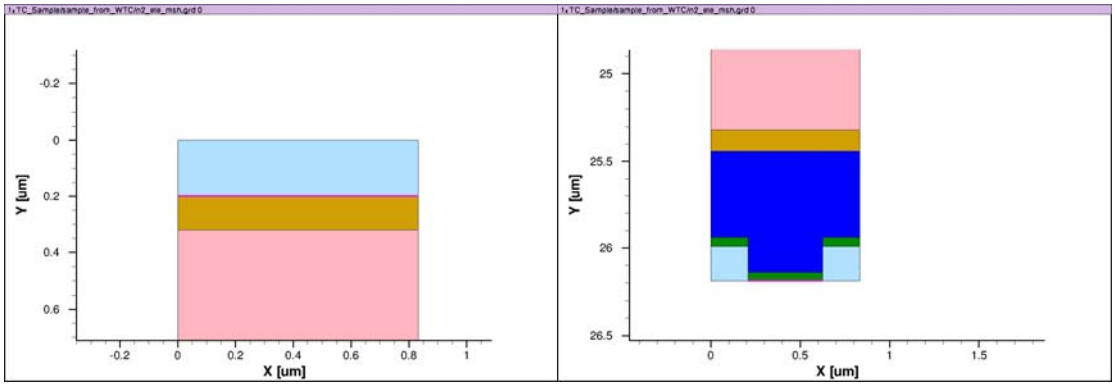

Figure 1. Structure demonstration of AlPO device calculation. (a) top part: gas, Si_3N_4, Silicon; (b) bottom part: Silicon, Si_3N_4, AlPO grid, gas.

After the structure is created, the generated mesh and doping information are stored in a TDR format file, which is then passed to Sentaurus Device.

(2). Sentaurus Device: Calibration.

In this node, the voltage on the AlPO terminal called “gate” is biased to 1 V in the “Solve” section of the input file, and the mobility is monitored at 1 nm below the AlPO–Si_3N_4 interface as specified in the “CurrentPlot” section.

Since there is no current through the device, the continuity equations are not solved. The setup uses the Philips unified mobility model, quantum potential, and mobility degradation at the silicon–dielectric interface, which are accounted for in the Lombardi_highk model. The latter model accounts for the RPS and RCS contributions due to the scattering in the vicinity of the AlPO interface. A modified version of the model is used here. Its parameterization is the same as in Lombardi_high-k model described in the Sentaurus Device User Guide.

The model used here contains a contribution limiting the RPS and RCS effects to the regions close to the interface; the mobility automatically approaches the bulk values at distances far from the interface. I changed the default parameter, for example, the RCS contribution to the total mobility given by:

$$\frac{1}{\mu} = \frac{1}{\mu_{Lombardi}} + \frac{\alpha_{rcs}}{\Delta\mu_{rcs}} + \frac{\alpha_{rps}}{\Delta\mu_{rps}} \tag{1.7}$$

It can be simplified to:

$$\Delta\mu_{rcs} = \mu_{rcs}\left(\frac{N_A}{3*10^{16}}\right)^{\gamma_1} \frac{N_s}{10^{11} cm^{-2}} \tag{1.8}$$

Here, N_A is the acceptor density and Ns is proportional to the perpendicular electrical field. Also, the RPS contribution is unchanged:

$$\Delta\mu_{rps} = \mu_{rps}\left(\frac{E_{\perp}}{10^6 V/cm}\right)^{\gamma_5}\left(\frac{T}{300K}\right)^{\gamma_6} \tag{1.9}$$

Using standard Inspect commands in the Inspect node of the Sentaurus Workbench project, the Philips model, Lombardi model, RCS, RPS, and the total mobility contributions are presented in Figure 2.

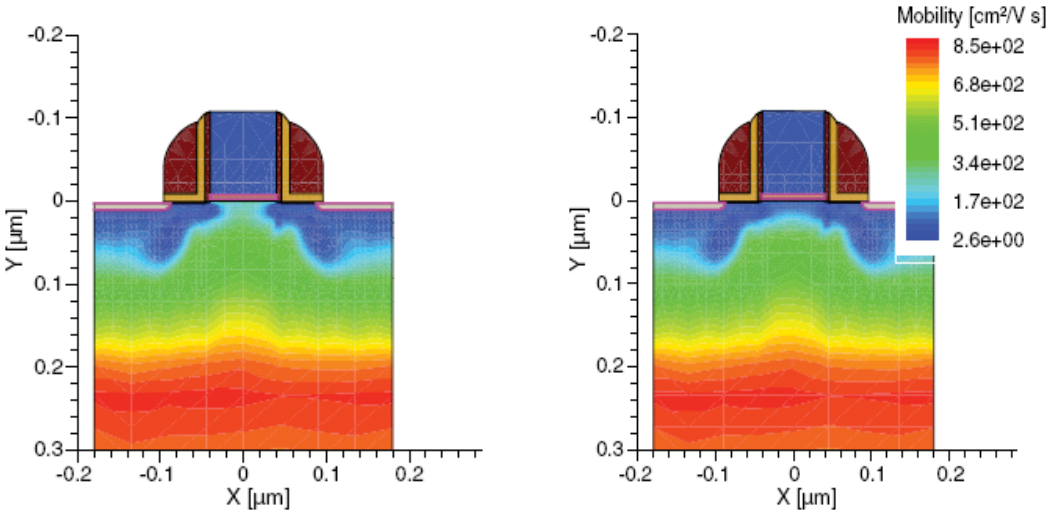

Figure 2. Mobility distribution without high-k model (left), and with high-k model (right), obtained with Vd = 50 mV, Vg = 1 V.

Noting that the slope of the mobility at low field is controlled by the RCS contribution; whereas, the high-field level is controlled by the Lombardi model and RPS contributions. Therefore, setting $\mu_{rcs} = 50$ and $\gamma_1 = 0.6$, we can obtain the slope corresponding to the experimentally observed one, while the default Lombardi and RPS parameters give the necessary high-field values.

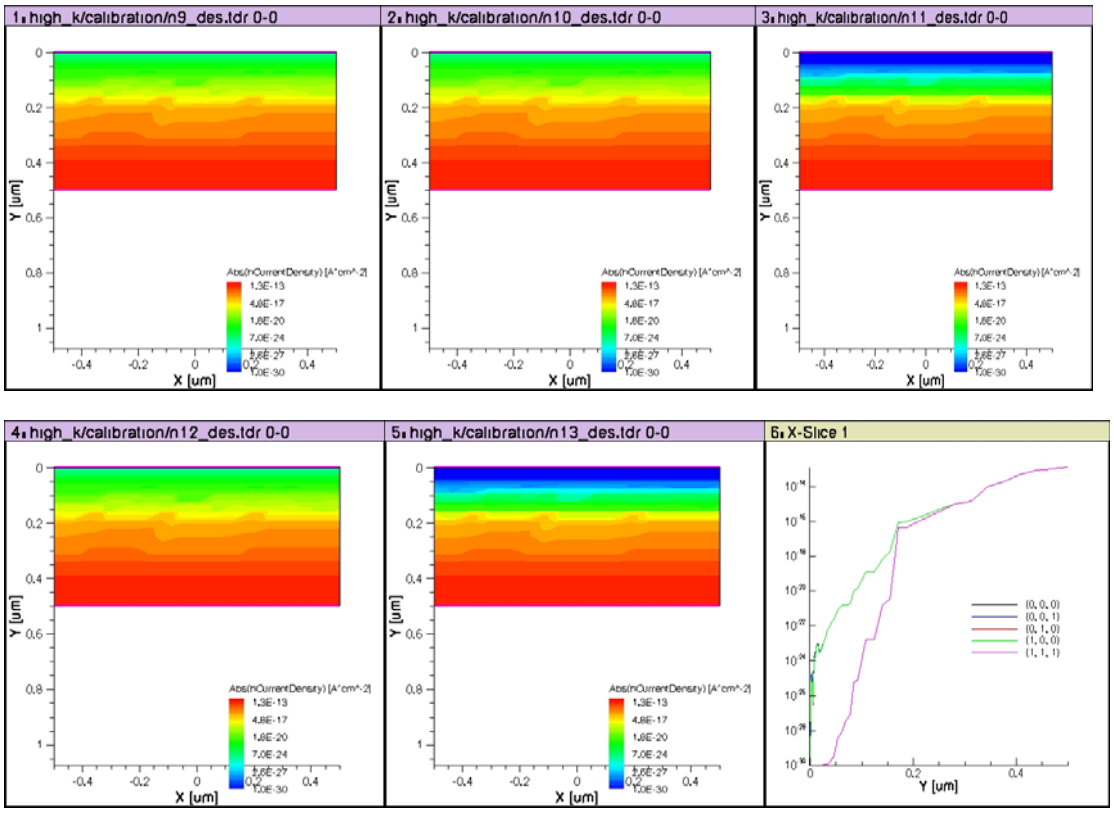

Figure 3. Absolute hole current density in different cases. (a) No Lombardi, No RCS, No RPS; (b) No Lombardi, No RCS, Have RPS; (c) No Lombardi, Have RCS, No RPS; (d) Have Lombardi, No RCS, No RPS; (e) Have Lombardi, Have RCS, Have RPS; (f) x-cut at x=0.4 um.

From Figure 3(6), we can see that the curve is only different when we change RCS from close to open, it doesn't matter whether we change Lombardi or RPS cases. This suggests that the device is in strong inversion mode, in which case the RCS-limited mobility becomes higher, since screening effect becomes larger at higher carrier density and at higher temperature.

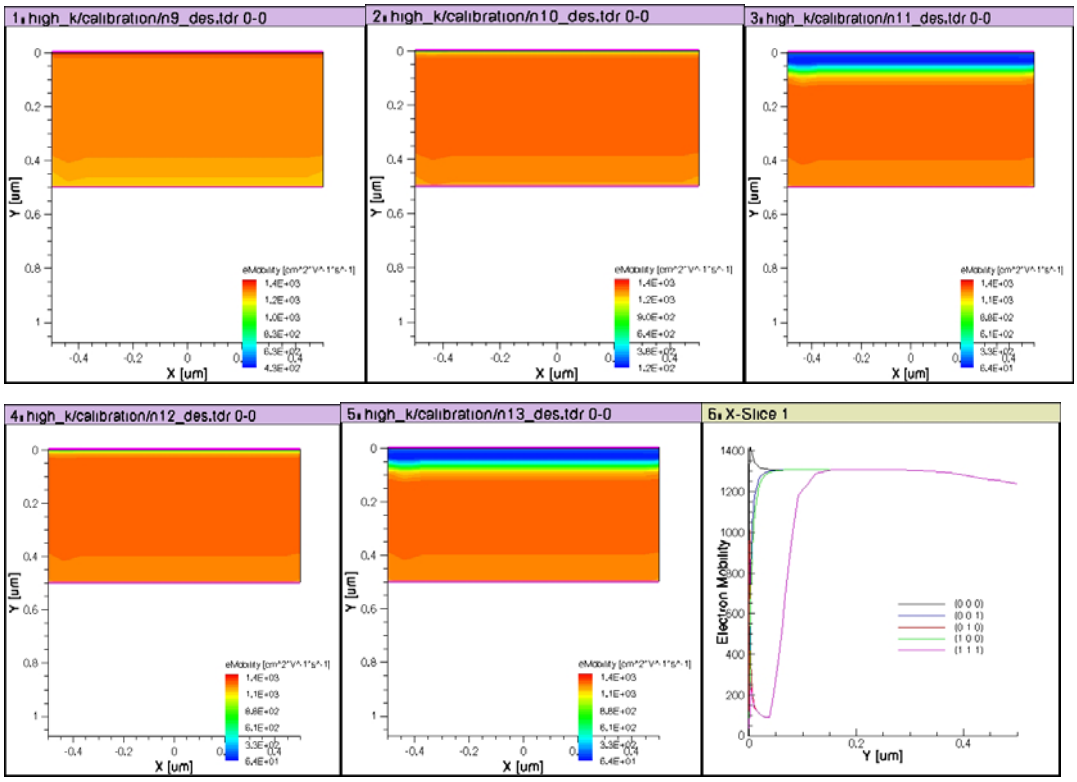

Figure 4. Electron mobility versus width for Sentaurus device simulation. (a) No Lombardi, No RCS, No RPS; (b) No Lombardi, No RCS, Have RPS; (c) No Lombardi, Have RCS, No RPS; (d) Have Lombardi, No RCS, No RPS; (e) Have Lombardi, Have RCS, Have RPS; (f) x-cut at x=0.4 um.

We can see from Figure 4(6) that, the electron mobility is only different in the interface area. The interface electron mobility is strongest if we turn off Lombardi, RCS and RPS, as shown in the black curve. The difference between (3) and (5) is the smallest, with (3) having a much stronger peak at interface area. The curve of (3) and (5) matches perfectly when Y > 0.04 um. This phenomenon suggests that the difference of RCS is the most important one within all these 3 differences. Also, curve (2) and (4) match perfectly, which indicates that the difference of RPS is the least important one within all these 3 differences.

In conclusion, the significance of all these three difference can be ranked as below:

Remote Coulomb scattering (RCS) >> Lombardi > Remote phonon scattering (RPS).

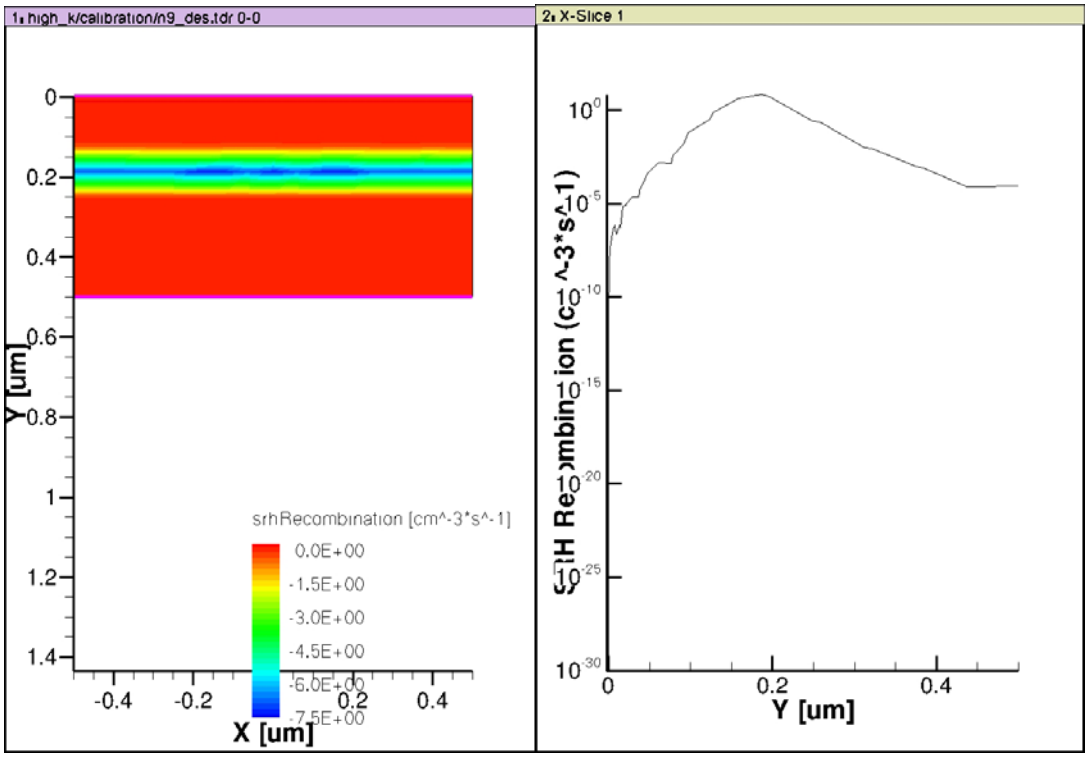

Figure 5. (a) SRH recombination rate versus depth; (b) x-cut at x=0.4 um.

This Schottky-Read-Hall recombination rate is kind of strange to me. It has a trough at the depth of about 0.2 um. But from depth = 0 to 0.5 um, all the material is just silicon, which indicates that there is a though of SRH recombination rate in the middle of silicon region.

2. Part II: Effect of high-k mobility degradation in MOSFET

This part of the project mostly repeats the setup of the device simulation from another application note. The project is modified to focus on the high-k mobility effects in the following way: The process simulation is removed from the setup. Results of the process simulation of the NMOS and PMOS devices with a gate length of 80 nm from the project are used as the input for the device simulation. The respective NMOS and PMOS structures are contained in the nMOS_gl80nm.tdr and pMOS_gl80nm.tdr input files. In the Sentaurus Device part, modifications related to the high-k mobility model have been made.

In the Sentaurus Device nodes, the parameter files include the section setting the parameters for the Lombardi_highk_v2 model, the PMI path is set with the command pmipath="@pwd@", and the following line is added to the Mobility section:

$$\text{Enormal(Lombardi\_highk\_v2)} \qquad (1.10)$$

The Sentaurus Workbench parameter highk is introduced to switch the RPS and RCS contributions on and off through the model parameters:

alpha_rcs_e = @highk@
alpha_rcs_h = @highk@
alpha_rps_e = @highk@
alpha_rps_h = @highk@ (1.11)

A simulation is performed only for the gate length of 80 nm. Therefore, the Inspect node “rolloff” is removed from the setup.

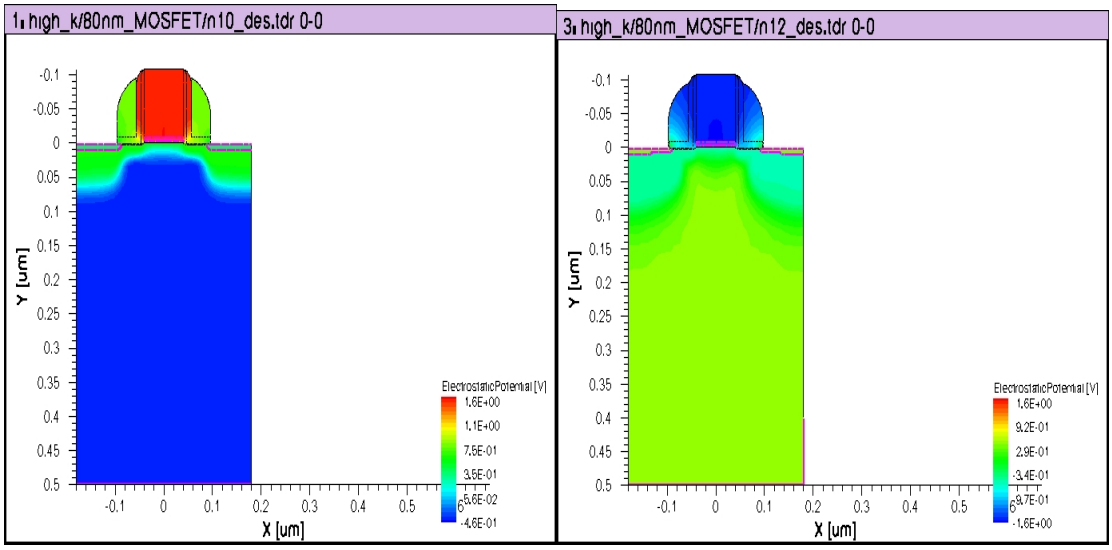

Figure 6. ElectroStatic Potential in (a) nMOS; (b) pMOS.

Figure 6 shows the electrostatic potential of the nMOS and pMOS built using the materials above. We can see that the potential line has a plateau around the gate area. It’s because all the potential difference is added from gate, due to the limit length of gate area, the potential is higher / lower near gate area for nMOS / pMOS device.

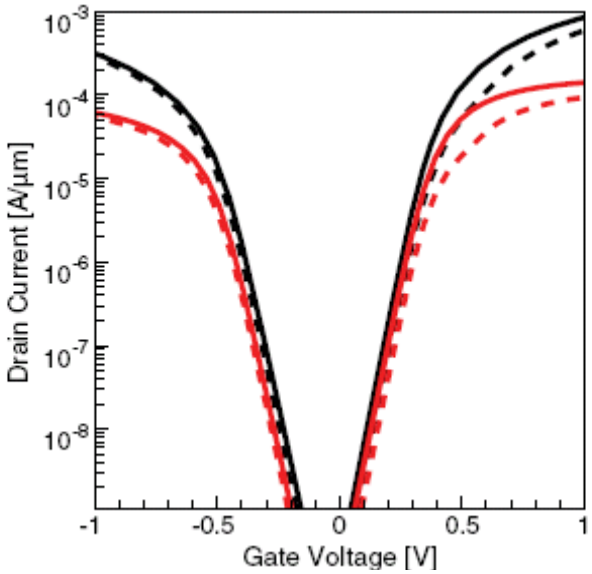

Figure 7. Drain current versus voltage on the gate for PMOS and NMOS with 80-nm gate length; dashed lines correspond to simulation with high-k model and solid lines correspond to simulation

without high-k model: Vd = 1 V (black) and Vd = 50 mV (red)

Figure 7 shows the typical mobility distribution in the device with and without the high-k model. As we can see, close to the gate region, the mobility is reduced when the high-k model is included. Corresponding to the mobility degradation in the channel region, the drain current is reduced when the high-k mobility model is included as seen in Figure 7.

Conclusion

These results prove that proper mobility modeling is important for quantitative simulation of the device characteristics. The versatility of the Sentaurus Device high-k mobility models such as aluminum nanoparticles allows for the simulation of various devices.

Reference

[1] Sentaurus Structure Editor User Guide
[2] Sentaurus Device User Guide
[3] Sentaurus Inspect User Guide
[4] Hiroyoshi Tanimoto, *et al*., “Modeling of Electron Mobility Degradation for HfSiON MISFETs”, in *International Conference on Simulation of Semiconductor Processes and Devices (SISPAD)*, Monterey, CA, USA, September 2006.